Unveiling Jet Collimation in M84: A High-Resolution VLBI Study of a Low-Luminosity AGN

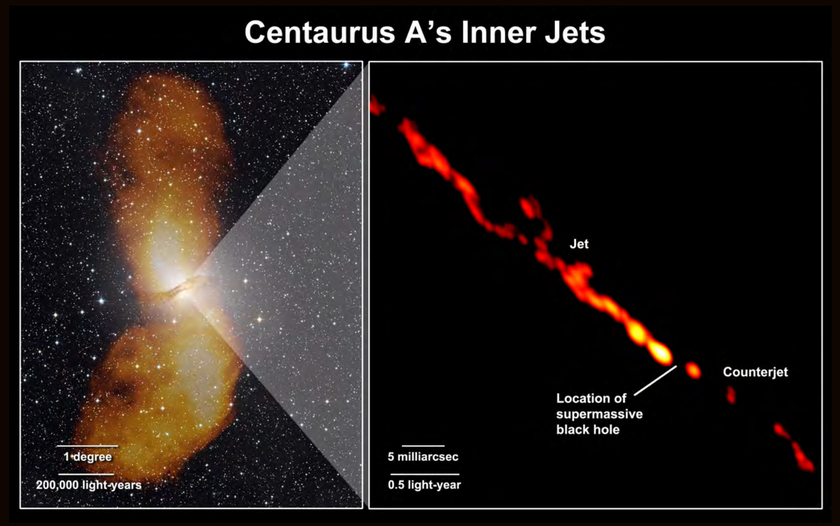
Elika Prameswari Fariyanto
(The University of Tokyo/NAOJ)

Collaborators: Kazuhiro Hada (Nagoya City University), Yuzhu Cui (Zhejiang Lab), Mareki Honma (The University of Tokyo/NAOJ), Masanori Nakamura (Hachinohe College/ASIAA), Keiichi Asada (ASIAA), Xuezheng Wang (Shanghai Astronomical Observatory), Wu Jiang (Shanghai Astronomical Observatory)

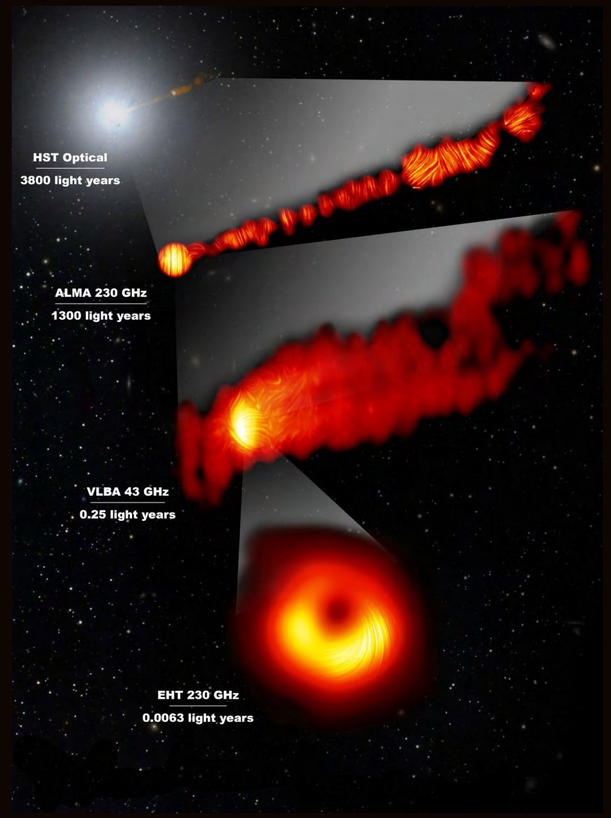
EAMA 11

Low-Luminosity AGNs

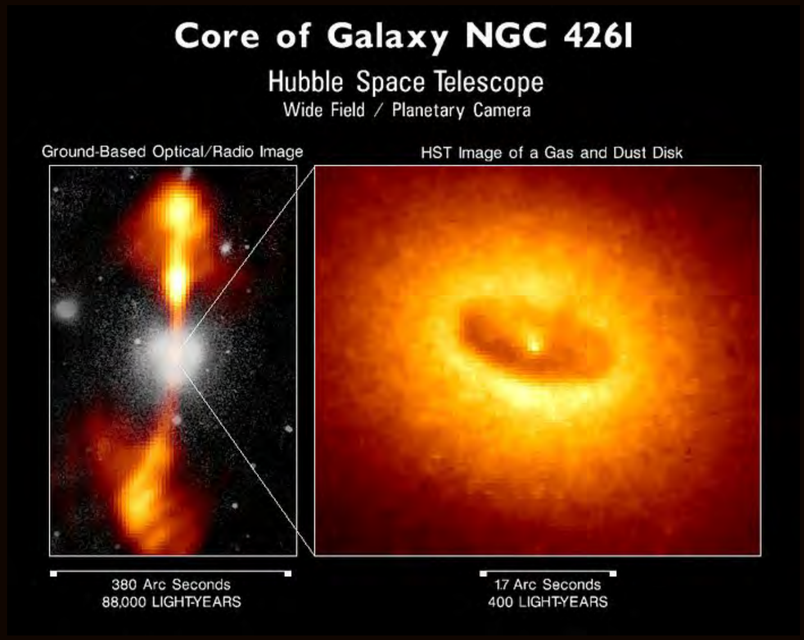
Cen A



M87



NGC 4261



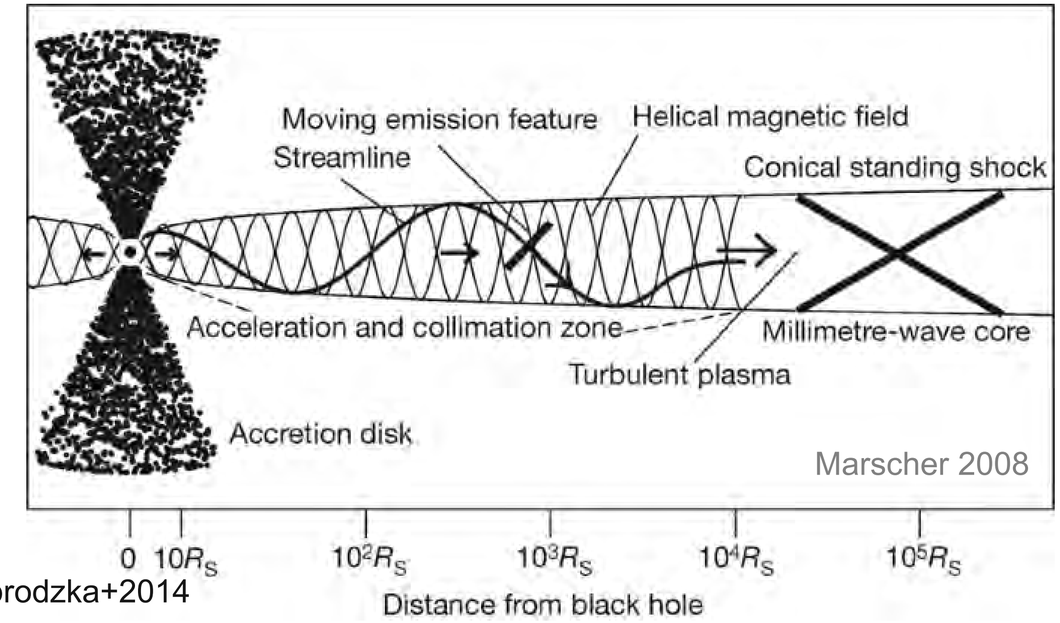
$L(H\alpha) \sim 2 \times 10^{39}\ \mathrm{erg\ s^{-1}}$ (Bower et al. 1997)

Example of widely studied sources

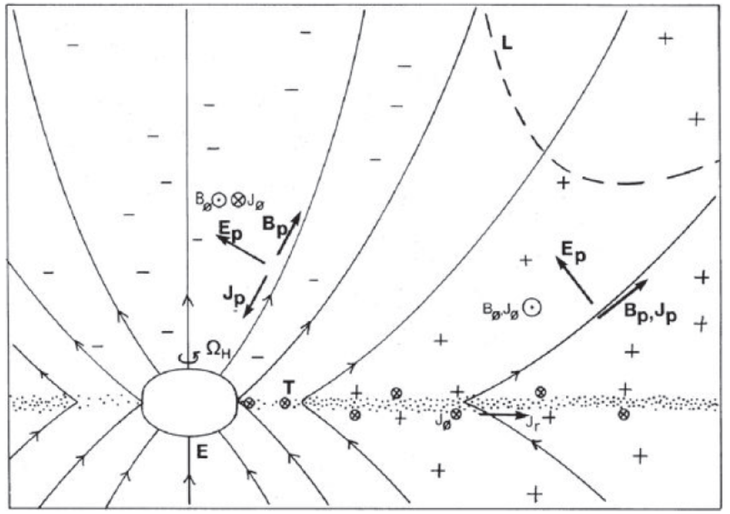
AGN jets key questions

1. How the jet production works?

2. How the jet is collimated and accelerated?



Mościbrodzka+2014



Blandford & Znajeck (1977)

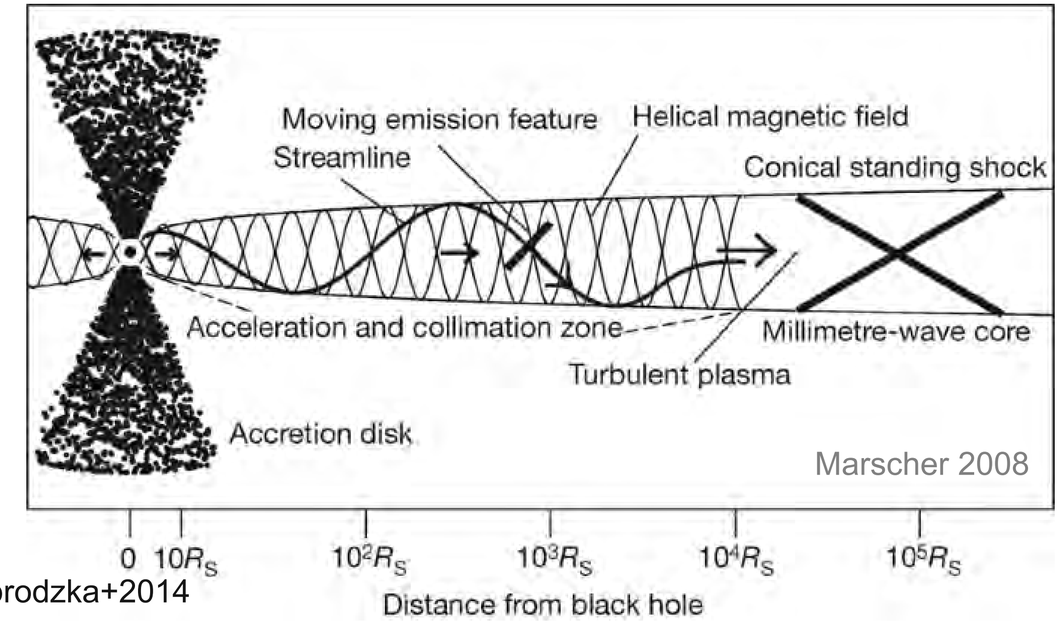
AGN jets key questions

1. How the jet production works?

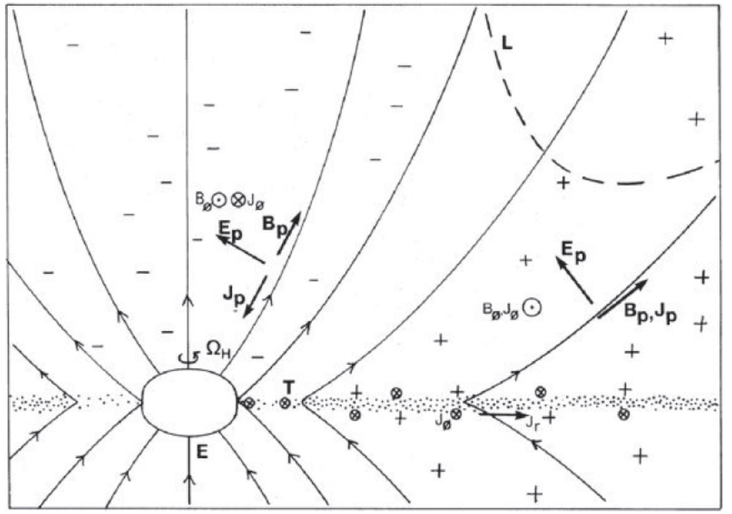
- Driven by energy extraction from the BH magnetic field through Blandford-Znajeck (1977) mechanism

2. How the jet is collimated and accelerated?

- Collimation by the wind/outflow from accretion disk (Blandford & Payne 1982)



Mościbrodzka+2014

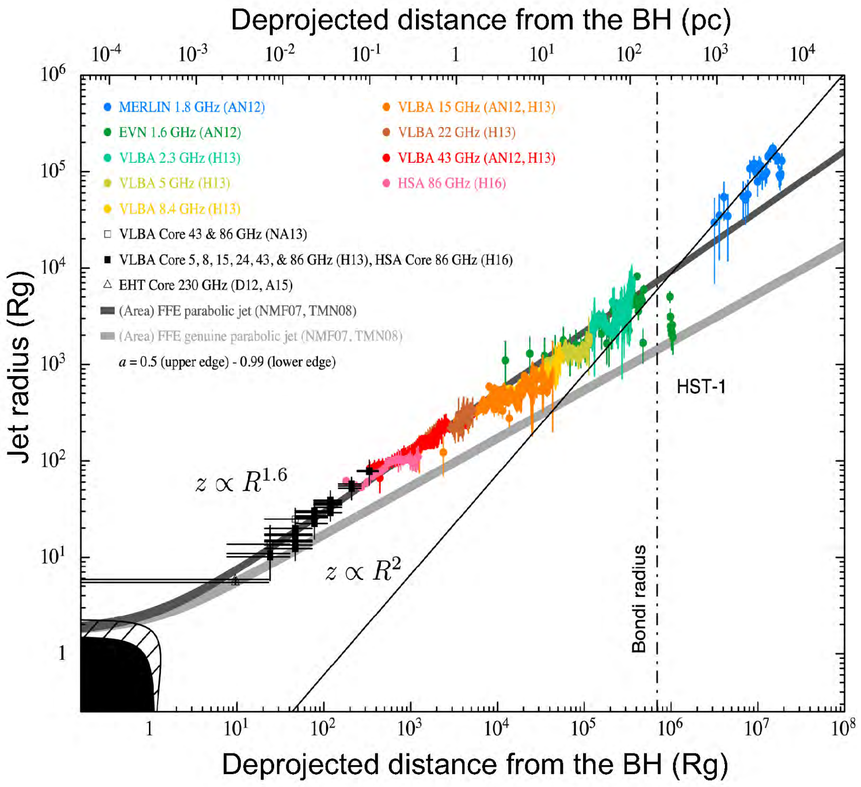


Blandford & Znajeck (1977)

Jet collimation profile

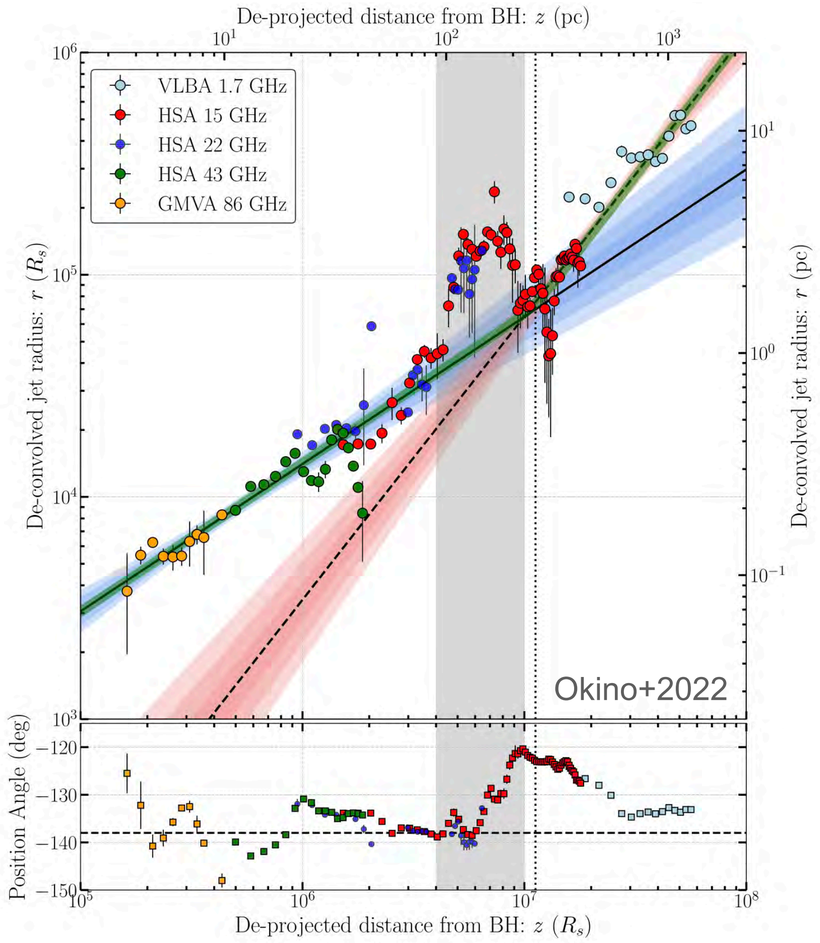
Observation using Very Long Baseline Interferometry (VLBI) are necessary

M87



Nakamura+2018

3C 273

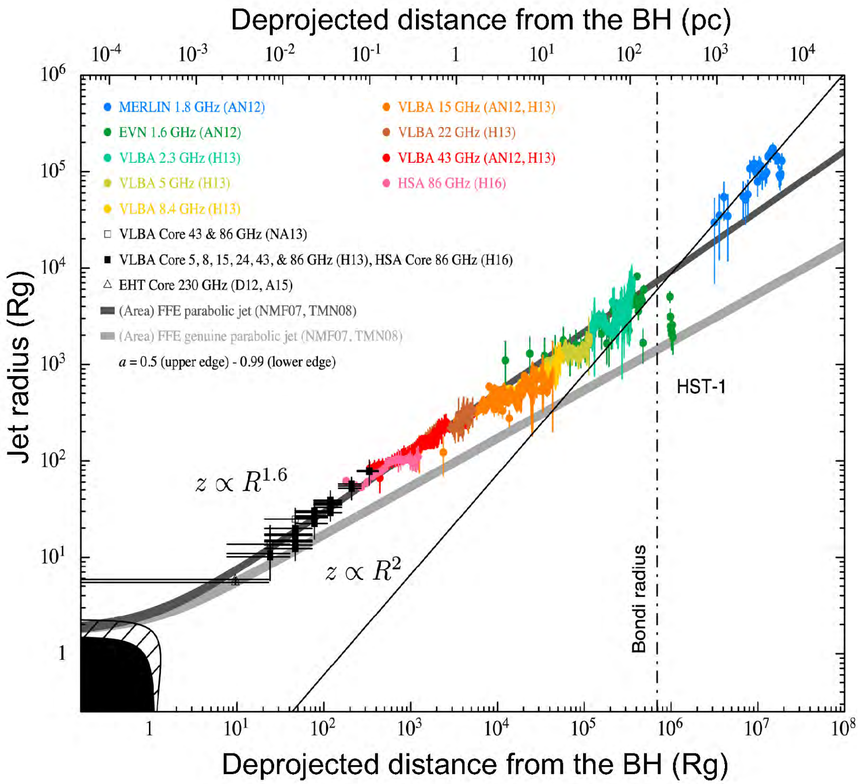


Jet collimation profile

Observation using Very Long Baseline Interferometry (VLBI) are necessary

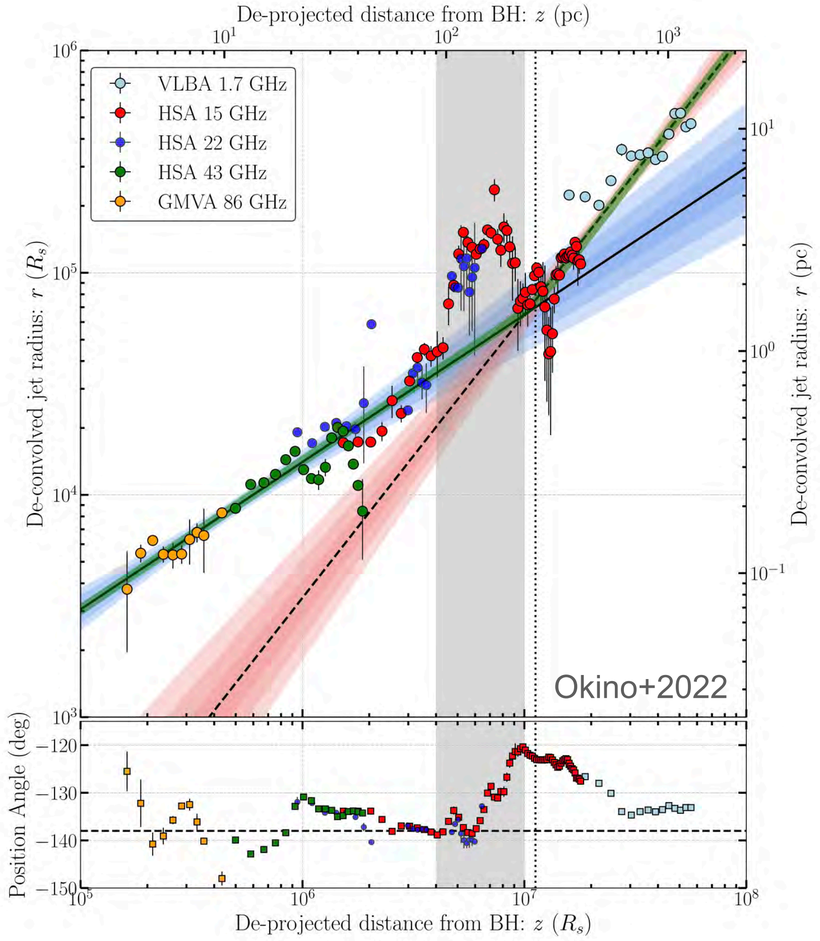
Previous studies of powerful jet sources: collimation break around or further than the Bondi radius or radius of gravitational influence

M87



Nakamura+2018

3C 273



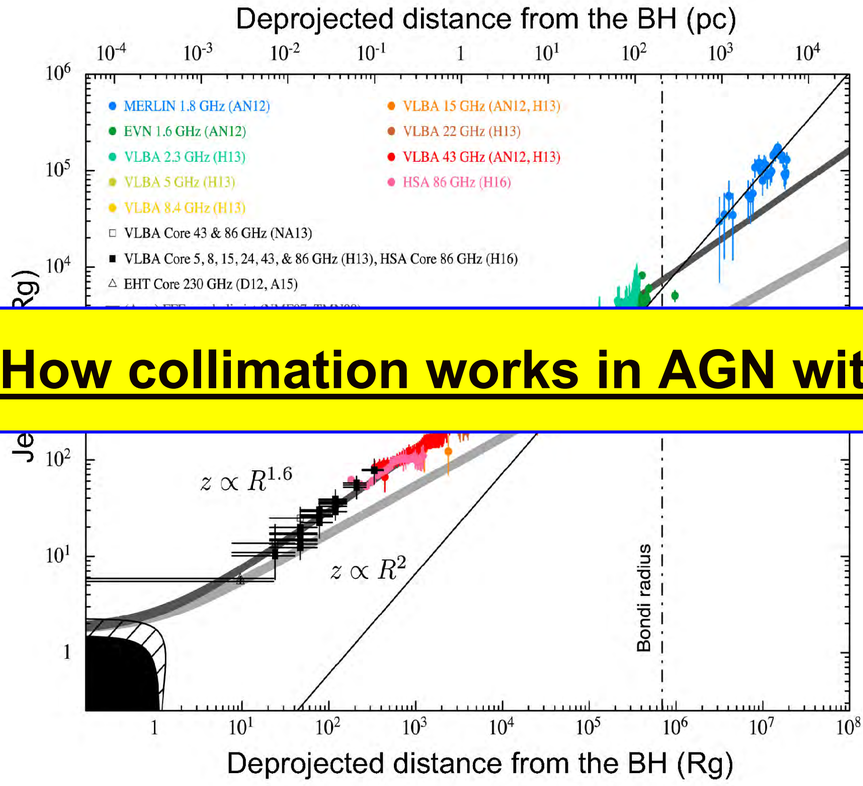
Jet collimation profile

Observation using Very Long Baseline Interferometry (VLBI) are necessary

Key question: How collimation works in AGN with lower-power jets?

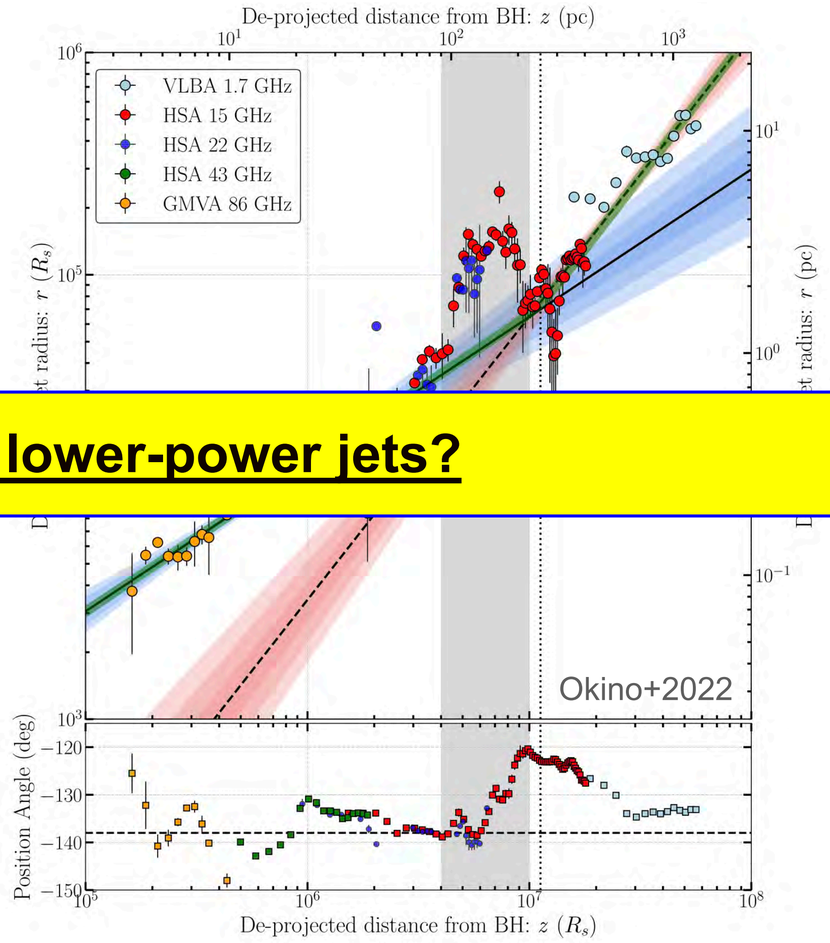
Previous studies of powerful jet sources: collimation break around or further than the Bondi radius or radius of gravitational influence

M87



Nakamura+2018

3C 273



M84

A nearby low-luminosity radio galaxy in Virgo cluster

(**Fanaroff-Riley I**)

$\boldsymbol{D = 16.83\ \mathrm{Mpc}}$, $\boldsymbol{\mathrm{M_{BH}} = 8.5 \times 10^{8}\ \mathrm{M_{\odot}}}$) Walsh+2010)

($1\ mas \sim 0.082\ pc \sim 10^{3}\ r_s$(



SDSS



SDSS/VLA/Chandra

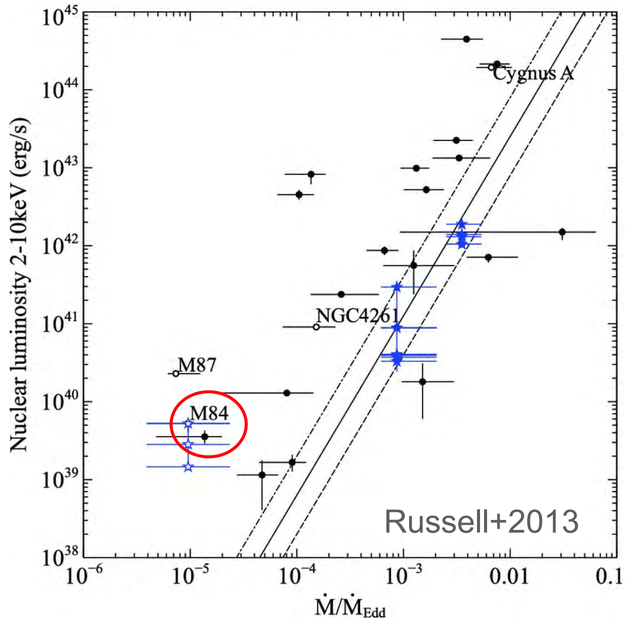
M84

A nearby low-luminosity radio galaxy in Virgo cluster

(**Fanaroff-Riley I**)

$\boldsymbol{D = 16.83\ \mathrm{Mpc}}$, $\boldsymbol{\mathrm{M_{BH}} = 8.5 \times 10^{8}\ \mathrm{M_{\odot}}}$) Walsh+2010)

($1\ mas \sim 0.082\ pc \sim 10^{3}\ r_s$(





SDSS



SDSS/VLA/Chandra

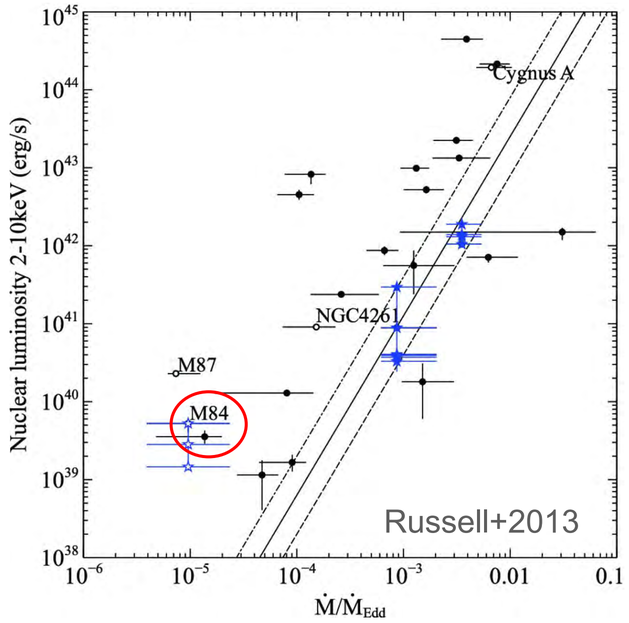
M84

A nearby low-luminosity radio galaxy in Virgo cluster

(**Fanaroff-Riley I**)

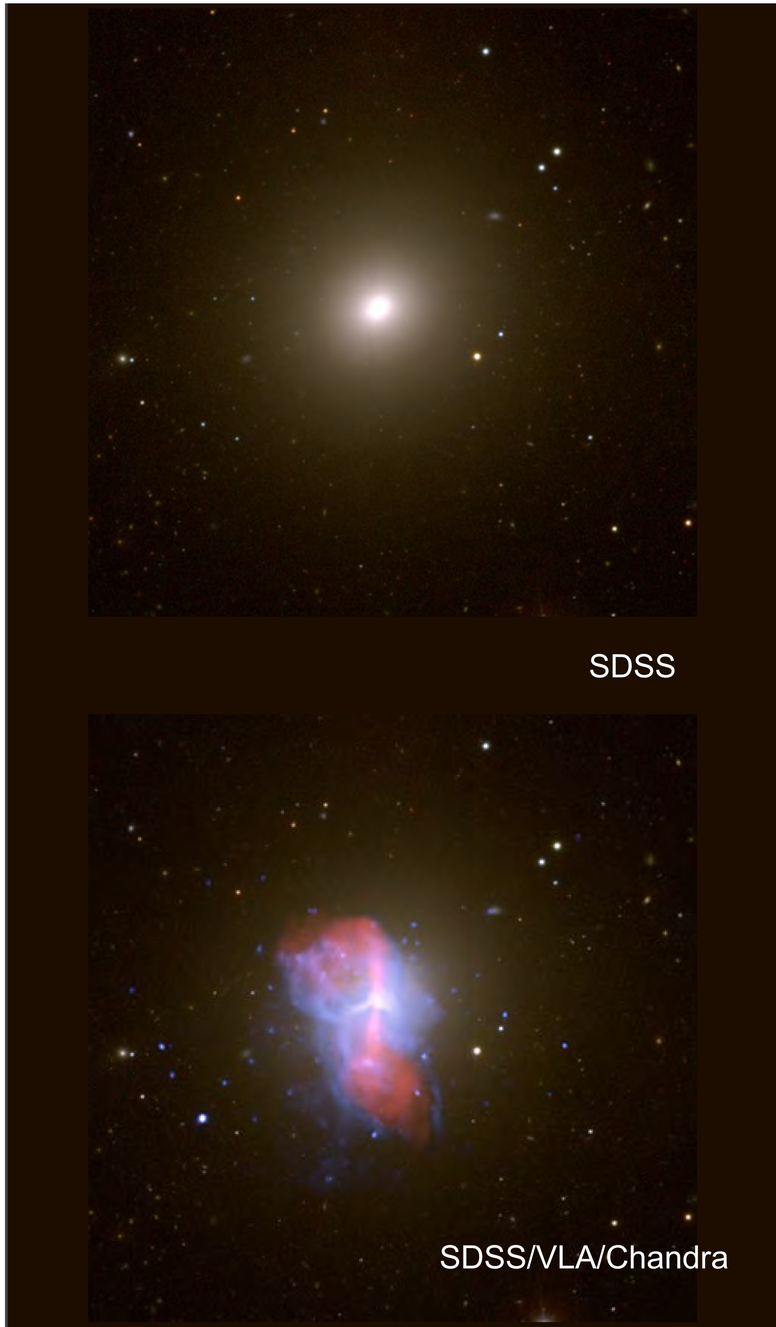
$\boldsymbol{D = 16.83\ \mathrm{Mpc}}$, $\boldsymbol{\mathrm{M_{BH}} = 8.5 \times 10^{8}\ \mathrm{M_{\odot}}}$) Walsh+2010)

($1\ mas \sim 0.082\ pc \sim 10^{3}\ r_s$(



Source name	$L_{Bol}\ (erg/s)$
M84	$\sim 1\times10^{41}$[1]
M87	$\sim 2.7\times10^{42}$[2]
NGC 4261	$\sim 4.0\times10^{42}$[3]
NGC 315	$\sim 1.9\times10^{43}$[4]
Cygnus A	$(0.5-2.0)\times10^{46}$[5]
3C 273	$\sim 10^{47}$[6]

[1] Bower+2000, [2] Prieto+2016, [3] Muñoz+2022, [4] Gu+1999, [5] Tadhunter+2003, [6] Paltani&Türler2005



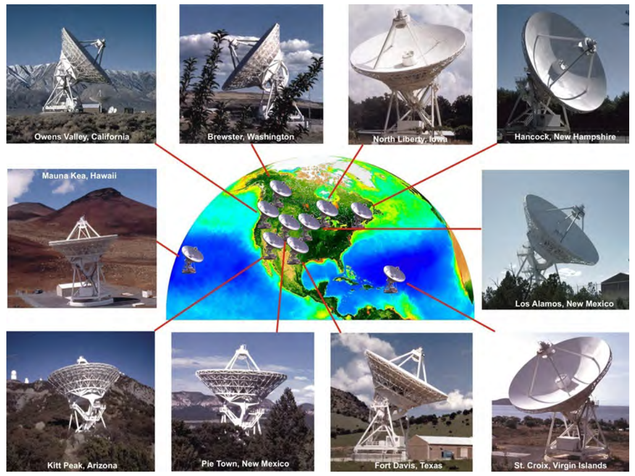
Observation data

➢ **Multi-frequency VLBA data**

Observation date: March 26, 2014

9 hrs continuous run of phase referencing observation

between M84 and M87 ($\Delta\theta \sim 1.5°$)



VLBA



VLA

Table 1. Multifrequency Radio Observations of M84

Frequency (GHz)	Band	Beam Size (mas × mas) (a)	I_p (mJy/bm) (b)	I_{rms} (mJy/bm) (c)
VLBA				
1.504	L	10 × 5	79.923	0.2345
4.996	C	3 × 1.5	109.980	0.1416
8.432	X	2 × 1	103.610	0.6467
15.496	U	1 × 0.5	104.920	0.3374
23.896	K	0.7 × 0.35	109.420	0.4089
43.296	Q	0.34 × 0.17	93.532	0.7613
VLA				
1.413		3860 × 3860	151.930	1.160

Observation data

➢ **Multi-frequency VLBA data**

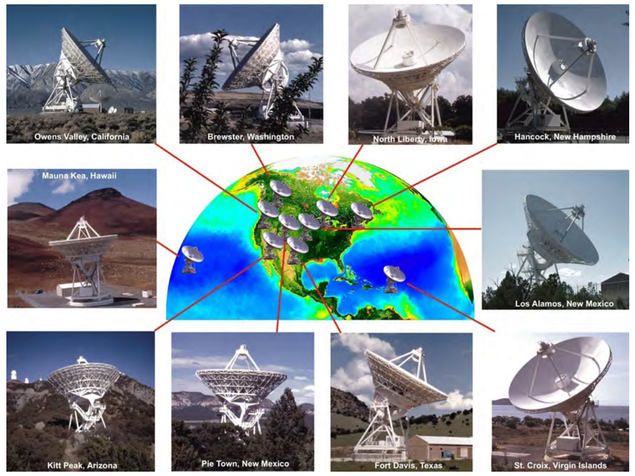
Observation date: March 26, 2014

9 hrs continuous run of phase referencing observation

between M84 and M87 ($\Delta\theta \sim 1.5°$)

➢ **Supplementary VLBA data** (Wang+2022)

Observation date: June 2, 2020 & March 31, 2021



VLBA



VLA

Table 1. Multifrequency Radio Observations of M84

Frequency (GHz)	Band	Beam Size (mas × mas) (a)	I_p (mJy/bm) (b)	I_{rms} (mJy/bm) (c)
VLBA				
1.504	L	10 × 5	79.923	0.2345
4.996	C	3 × 1.5	109.980	0.1416
8.432	X	2 × 1	103.610	0.6467
15.496	U	1 × 0.5	104.920	0.3374
23.896	K	0.7 × 0.35	109.420	0.4089
43.296	Q	0.34 × 0.17	93.532	0.7613
VLA				
1.413		3860 × 3860	151.930	1.160

Observation data

➢ **Multi-frequency VLBA data**

Observation date: March 26, 2014

9 hrs continuous run of phase referencing observation

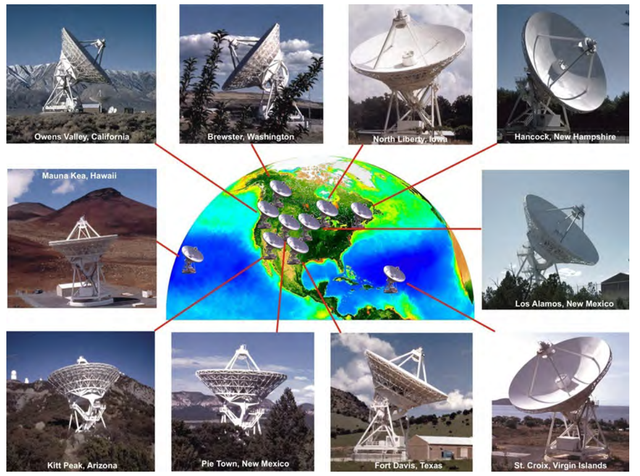
between M84 and M87 ($\Delta\theta \sim 1.5°$)

➢ **Supplementary VLBA data** (Wang+2022)

Observation date: June 2, 2020 & March 31, 2021

➢ **VLA Archival data** (Laing & Bridle 1987)

Observation date: November 9, 1980



VLBA

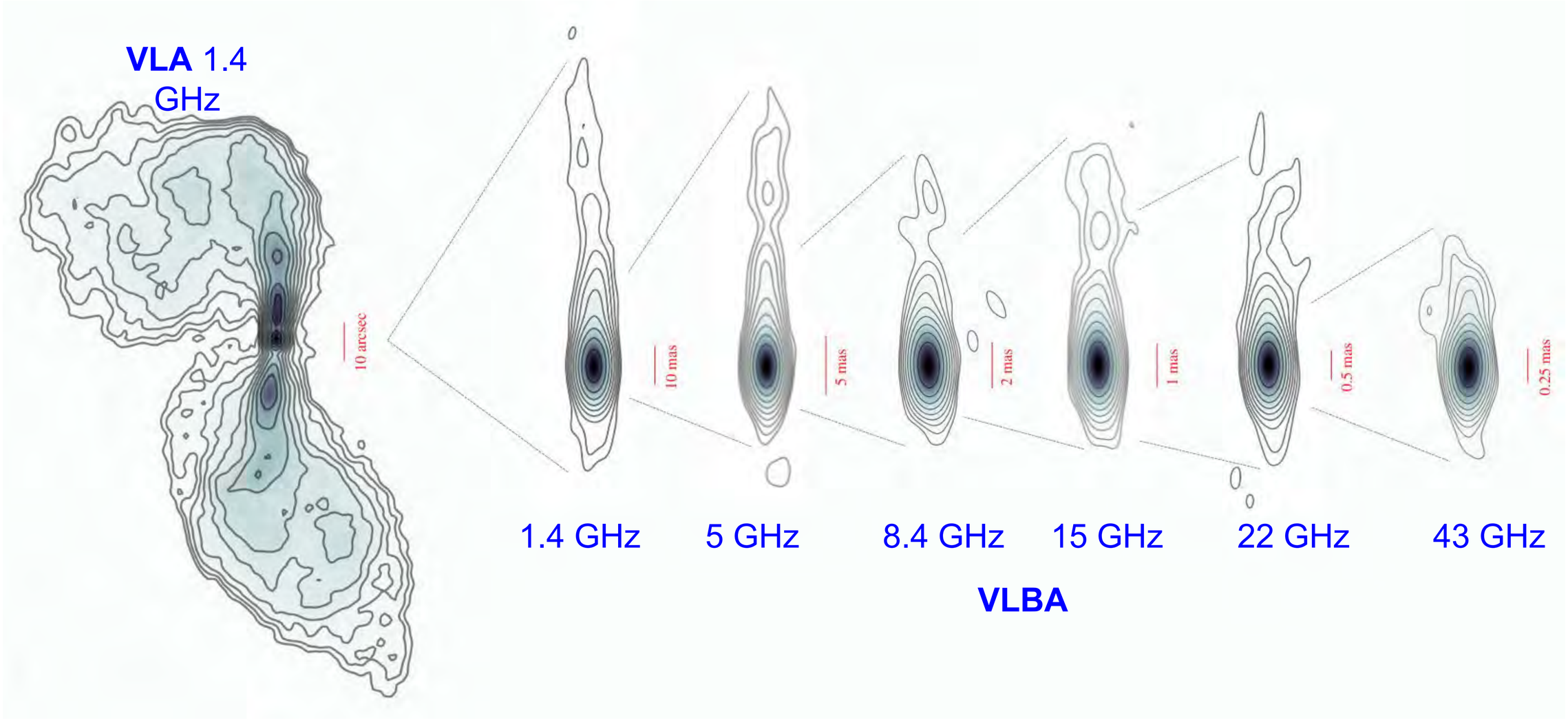


VLA

Table 1. Multifrequency Radio Observations of M84

Frequency (GHz)	Band	Beam Size (mas × mas) (a)	I_p (mJy/bm) (b)	I_{rms} (mJy/bm) (c)
VLBA				
1.504	L	10 × 5	79.923	0.2345
4.996	C	3 × 1.5	109.980	0.1416
8.432	X	2 × 1	103.610	0.6467
15.496	U	1 × 0.5	104.920	0.3374
23.896	K	0.7 × 0.35	109.420	0.4089
43.296	Q	0.34 × 0.17	93.532	0.7613
VLA				
1.413		3860 × 3860	151.930	1.160

Multi-frequency images



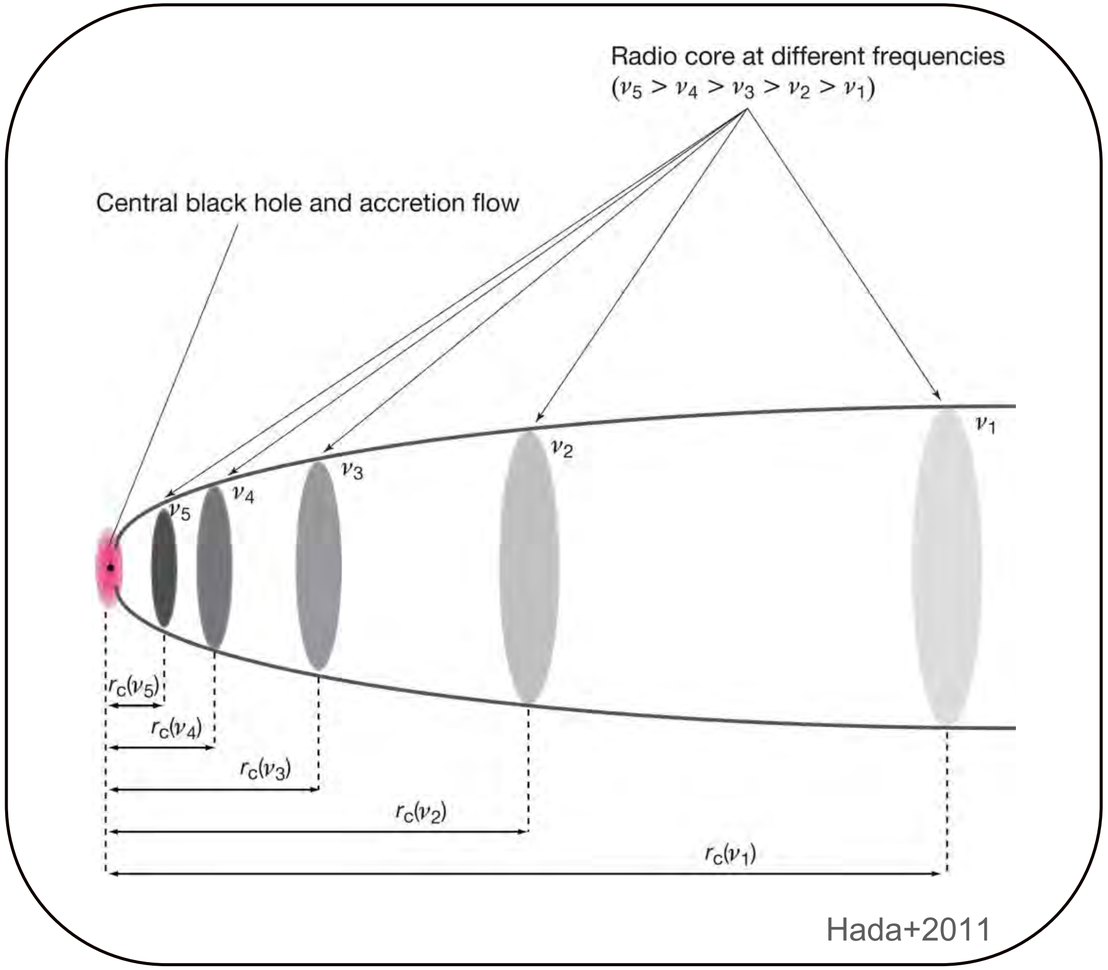
Core-shift concept

- At any given frequency, the VLBI core is observed at the location where the optical depth of synchrotron self–absorption is τ = 1.

- The separation between the central engine and a core at a given frequency ν satisfies
(e.g., Blandford & Königl 1979)

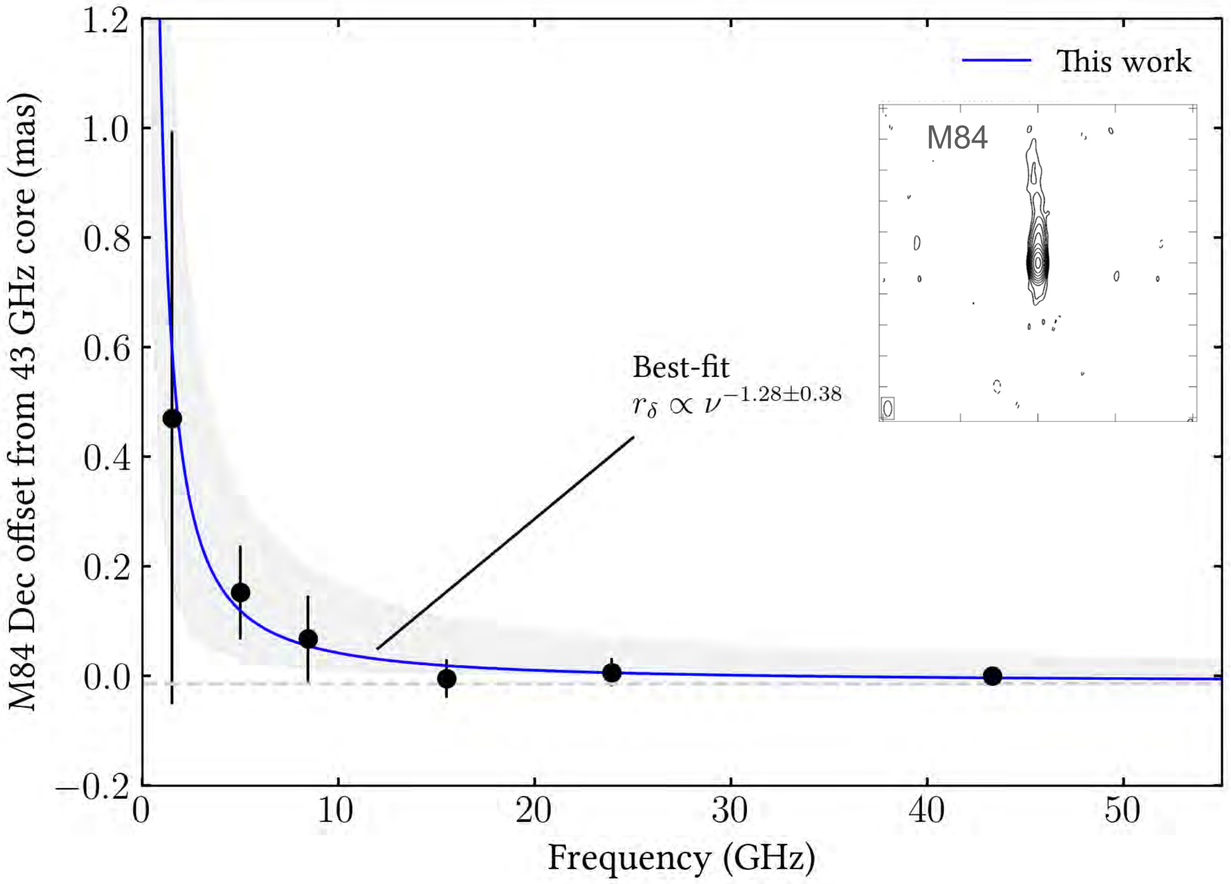
$$r_c(\nu) \propto \nu^{-\alpha} \quad (\alpha > 0).$$

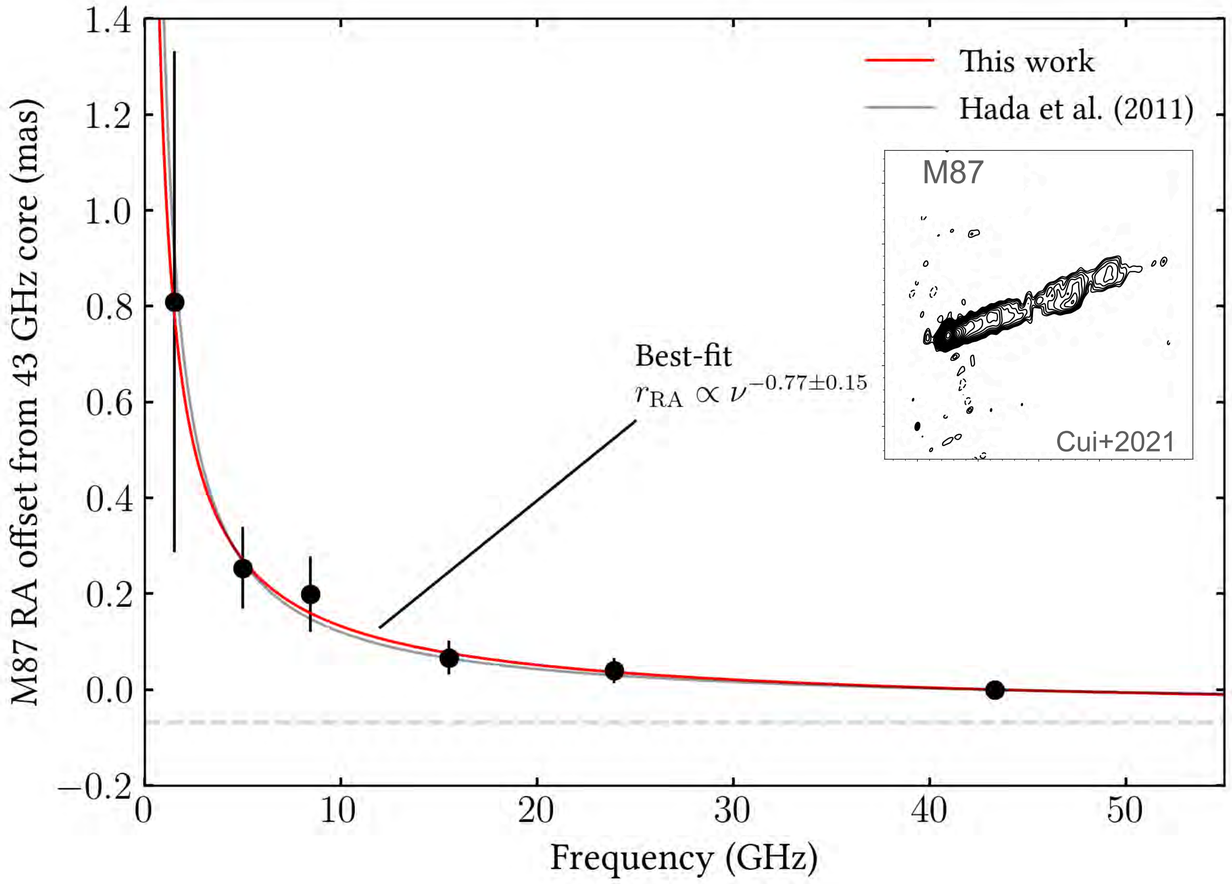
Core-shift measurement is important to precisely align multi-frequency images



Core-shift

Fariyanto et al. 2025

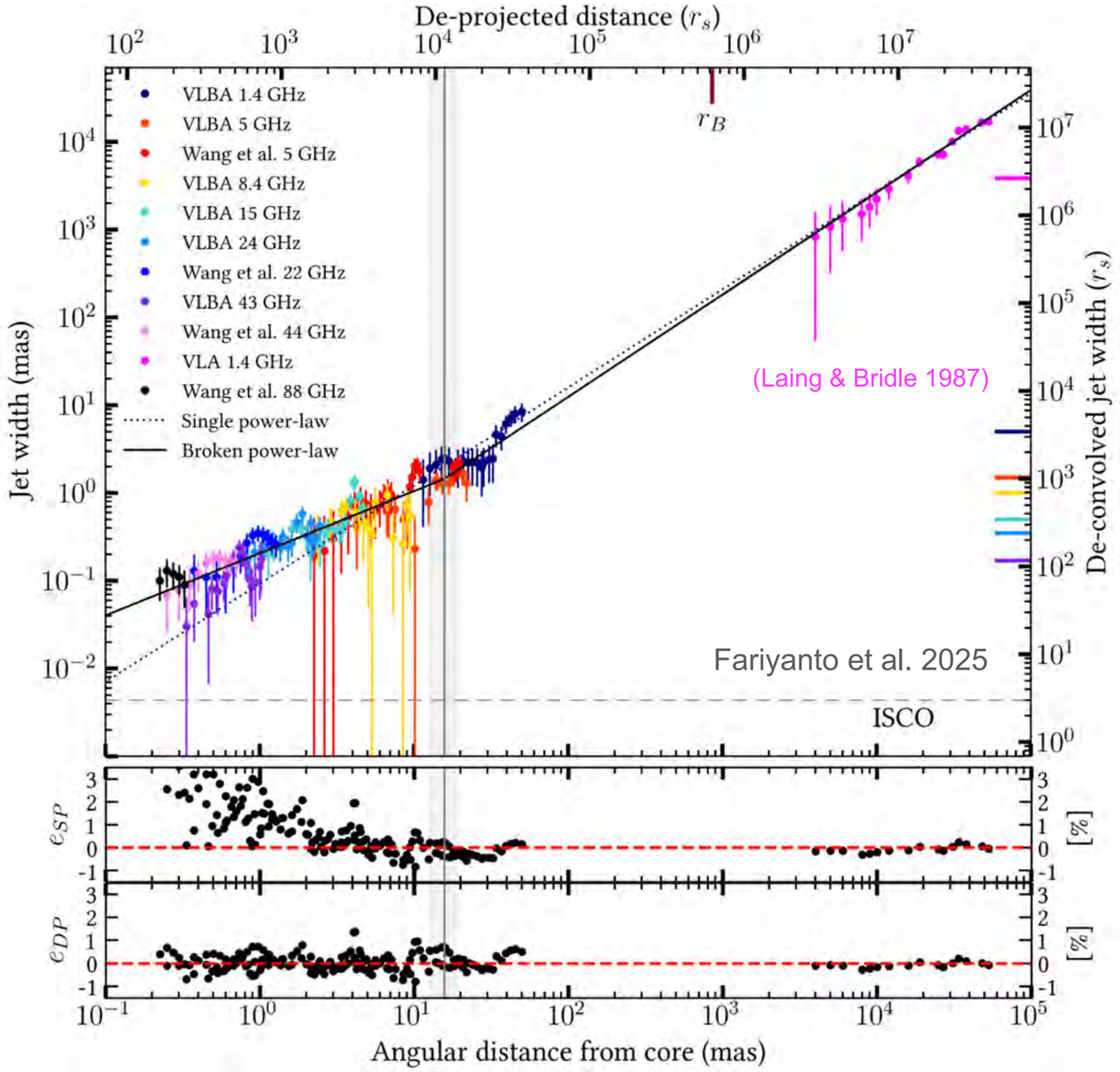




Jet collimation profile of M84

The M84 jet appears to follow parabolic geometry and later break into conical geometry

$$r_{break} \approx 1.67 \times 10^4 \, r_S$$



The jet is expanding rapidly even before it reaches the r_B

Jet collimation break and bondi radius

Bondi radius → spherical accretion where the matter becomes thermodynamically stable and satisfies virial equilibrium

$$r_B \simeq 6.2 \times 10^5 \, r_s \quad (\text{Bambic} + 2023)$$

Jet collimation break and bondi radius

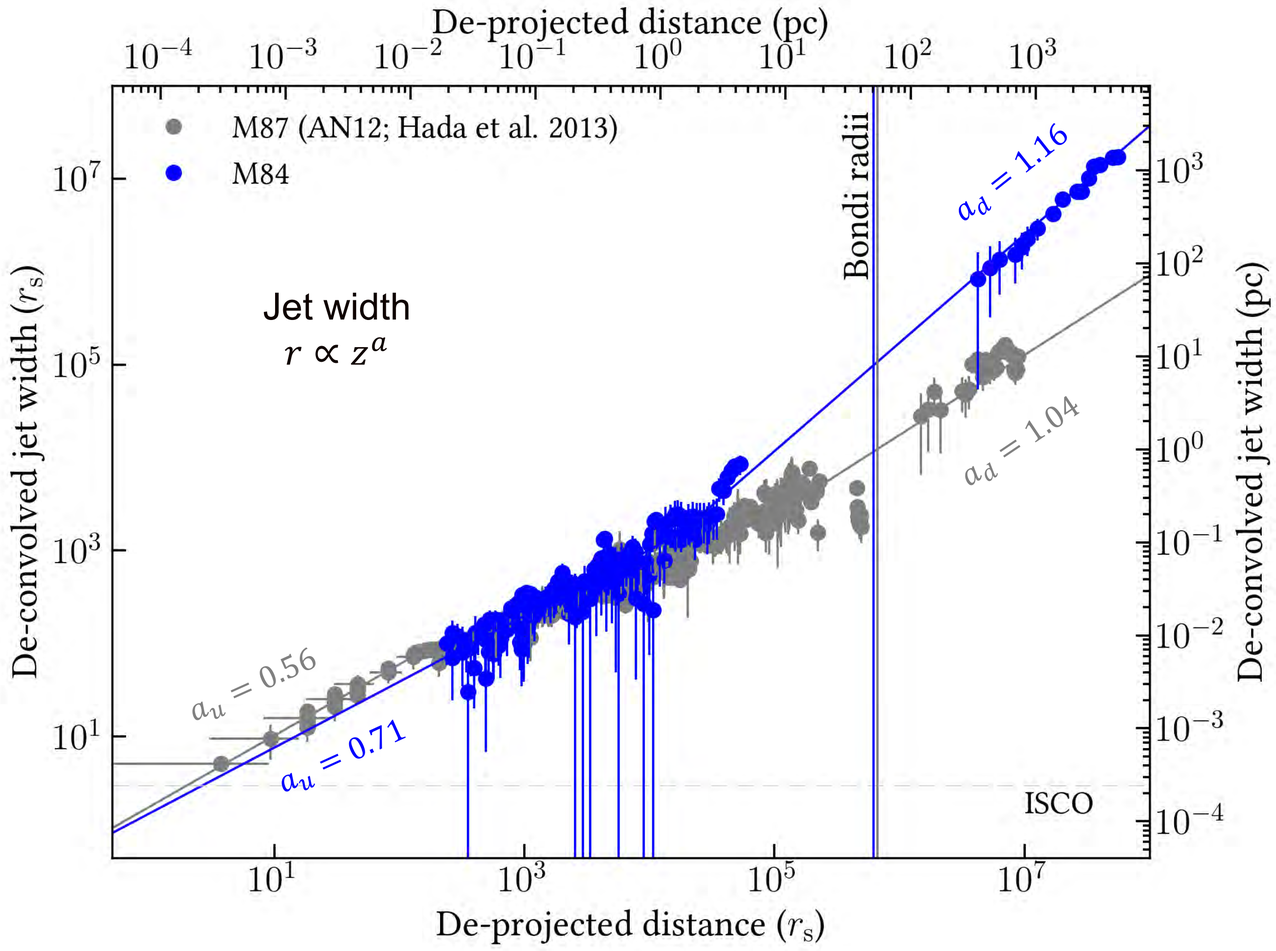
Bondi radius → spherical accretion where the matter becomes thermodynamically stable and satisfies virial equilibrium

$$r_B \simeq 6.2 \times 10^5 \, r_s \quad (\text{Bambic} + 2023)$$

What does it mean?

1. The transition at the Bondi radius is not universal
2. Possible rapid decrease in the density profile of material around the central engine

M84 vs M87



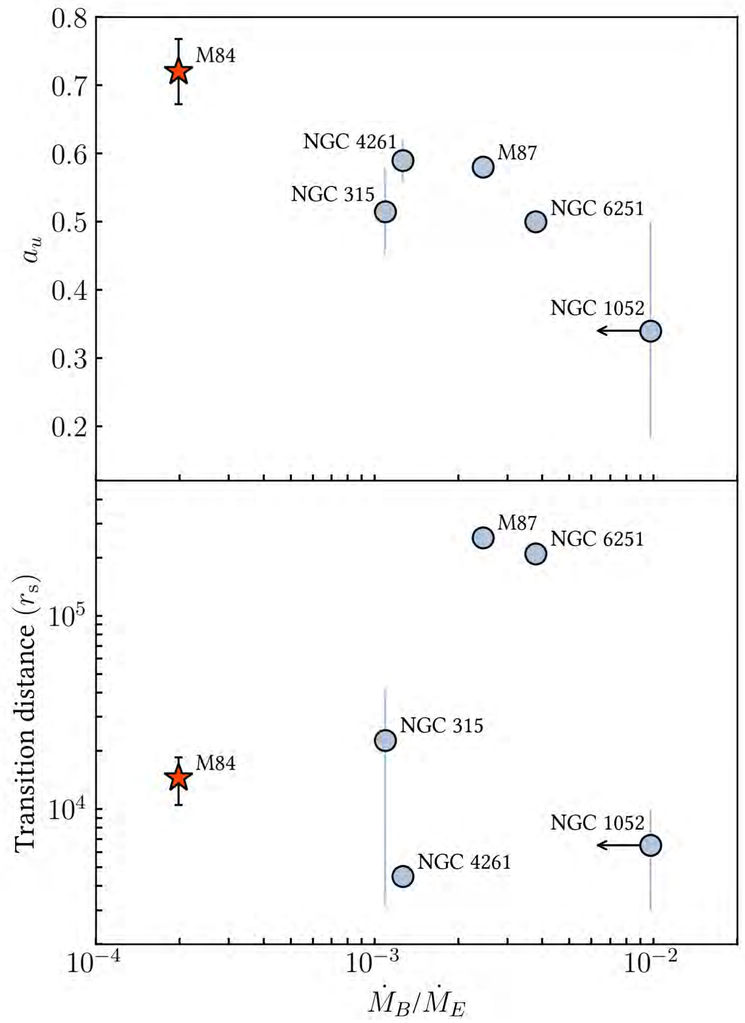
Fariyanto et al. 2025

- **Similarity:** Transition from parabolic to conical
- **Differences:** Wider jet width, position of transitional distance (M84: $r_{trans} \ll r_B$, M87: $r_{trans} \sim r_B$)

Why can this happen?

- Different environment around M84 jet → lower pressure density to hold the jet collimation

Comparison to other LLAGNs



Fariyanto et al. 2025

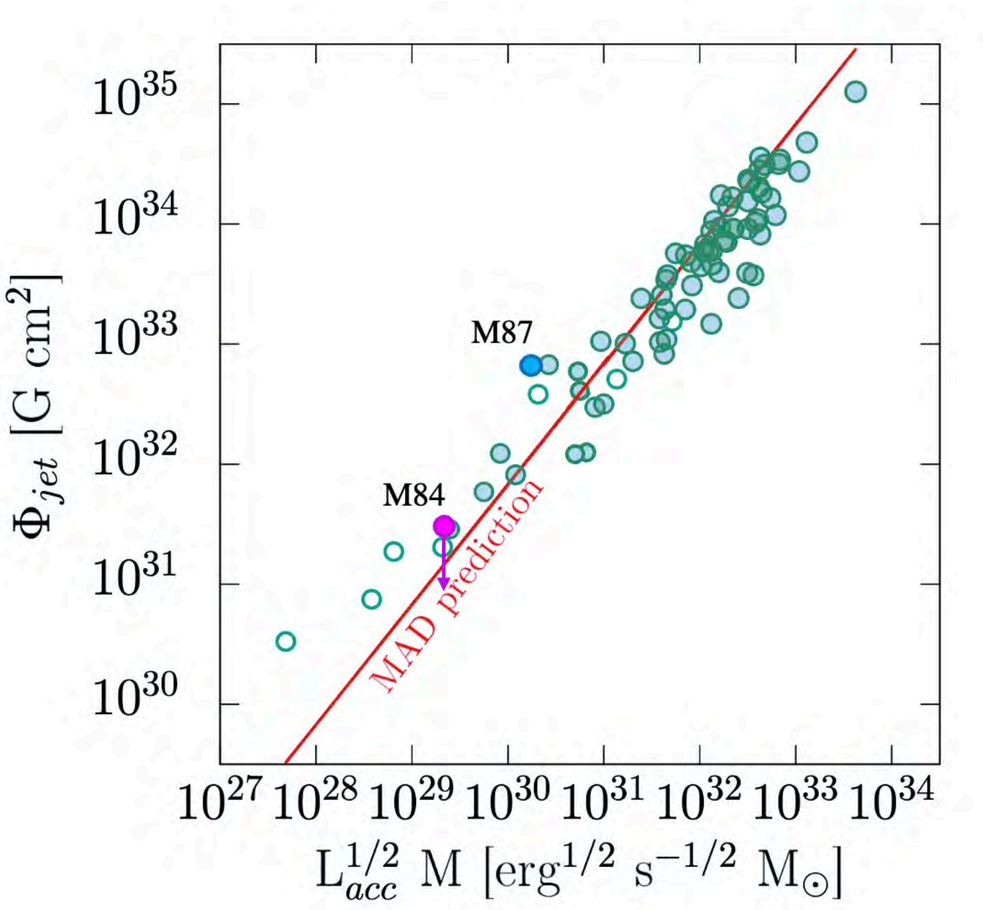
- According to theory and simulations, winds play a crucial role in confining jets (e.g., Komissarov+2009)
- Confinement in LLAGNs is attributed to external pressure provided by the disk wind from RIAFs with powers reaching up to $\approx 0.01\ \dot{M}c^2$ (Almeida & Nemmen 2020)
- LLAGNs with smaller $\dot{M}$ are expected to exhibit lower wind production rates → ineffective collimation with larger a_u and shorter transition distance.

Our study has begun to uncover clues about the controlling parameter of jet collimation (i.e. $\dot{M}$)

Magnetic field and flux

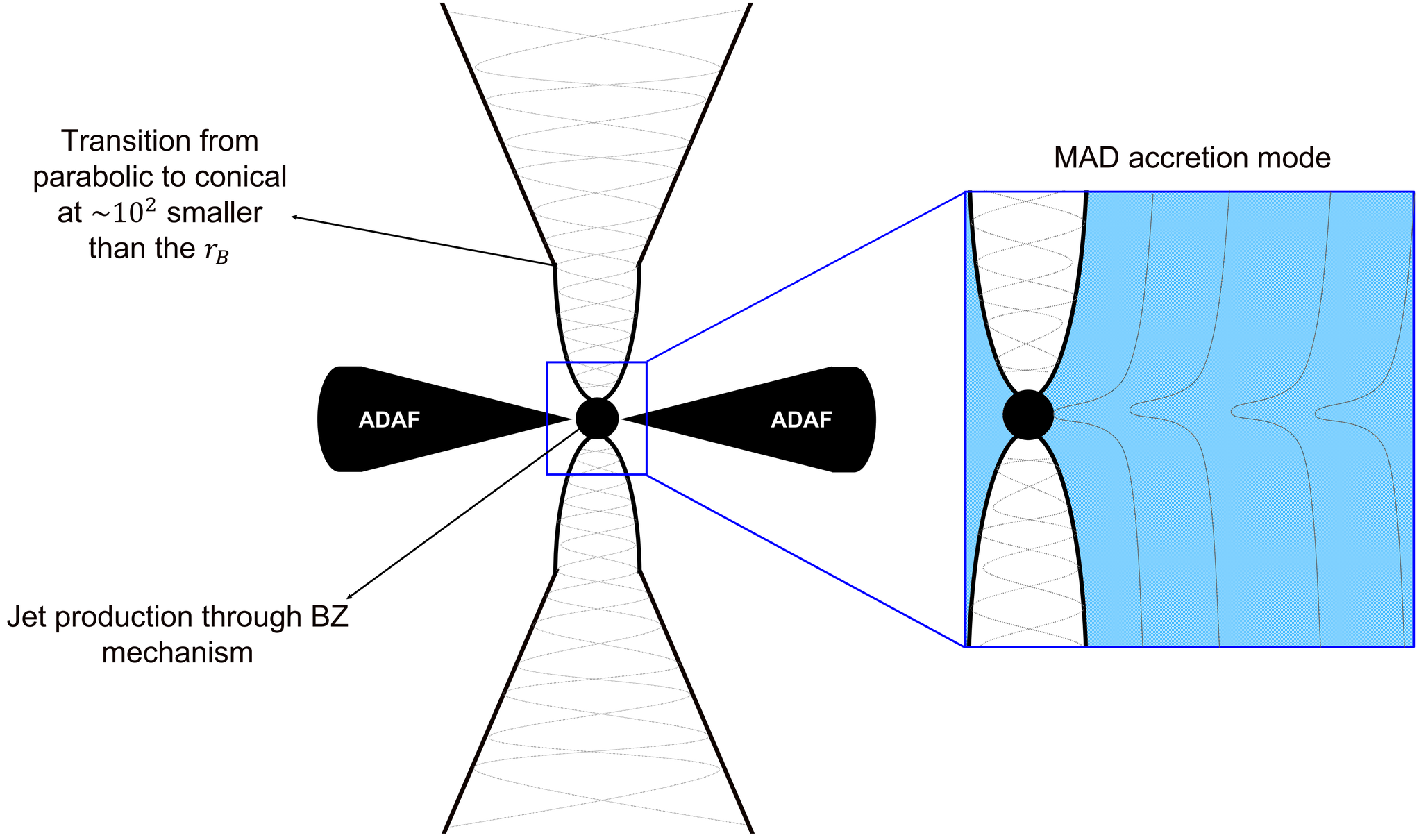
- Based on Lobanov (1998), we estimated the magnetic field at 1 pc from the jet base from the core-shift effect to be $\lesssim \mathbf{6.6\ mG}$
- Magnetic field strength at M84 core based on Synchrotron Self Absorption (SSA): $\mathbf{1{\sim}10\ mG}$ (Wang+2022)
- If we approximate the jet magnetic flux (Φ_{jet}) as Φ_{BH} for jets produced via BZ, we got $\lesssim \mathbf{10^{31}\ G\ cm^2}$

MAD scenario: magnetic field is important in very low luminosity jet sources



Adopted from Zamaninasab+2014, Chamani+2021

M84 jet model



Summary

- We found transition from parabolic to conical in M84 jet
- The transition almost $\sim 10^2$ smaller than the r_B
- Different case compared to M87 possibly due to different environment condition
- Magnetic field is important in M84 jet production
- We found a hint of a correlation between the observed jet collimation parameter and normalized accretion rate
- This suggests the importance of accretion activities in governing the LLAGN jet collimation mechanism

